

Comparison of superb microvascular imaging and  
contrast-enhanced ultrasonography for  
evaluation of intraplaque neovascularization  
in carotid arteries

Tetsuro KIYOKAWA<sup>1)</sup>, Kazumasa OURA<sup>1)</sup>, Takayuki CHIBA<sup>2)</sup>,  
Shunrou FUJIWARA<sup>2)</sup>, Ryo ITABASHI<sup>1)</sup>, Kuniaki OGASAWARA<sup>2)</sup>,  
Jiro HITOMI<sup>3)</sup> and Tetsuya MAEDA<sup>1)</sup>

<sup>1)</sup>Division of Neurology and Gerontology, Department of Internal Medicine,  
School of Medicine, Iwate Medical University, Yahaba, Japan

<sup>2)</sup>Department of Neurosurgery, School of Medicine,  
Iwate Medical University, Yahaba, Japan

<sup>3)</sup>Department of Anatomy, School of Medicine,  
Iwate Medical University, Yahaba, Japan

*(Received on January 10, 2023 & Accepted on February 14, 2023)*

Abstract

The purpose of this study was to compare the quantitative data of superb microvascular imaging (SMI) and contrast-enhanced ultrasonography (CEUS) as a method of identifying intraplaque neovascularization (IPN) in tissue specimens obtained by carotid endarterectomy. We enrolled 25 patients who underwent carotid endarterectomy because of  $\geq 70\%$  ipsilateral carotid stenosis. We evaluated intraplaque microvascular flow (IMVF) signals within carotid plaques by SMI and calculated the ratio of the difference between the maximum and minimum IMVF signal intensities ( $ID_{IMVF}$ ) to that of the lumen ( $ID_l$ ). We also measured contrast effects by CEUS and calculated the ratio of the difference

between maximum and baseline intraplaque intensities ( $EI_p$ ) to that of intraluminal curves ( $EI_l$ ). IPN number and area were measured on histological sections immunostained with anti-CD34 antibody. We identified IMVF signals in 8 patients and contrast effects in 12 patients. The  $EI_p/EI_l$  ratio was significantly correlated with IPN area ( $\rho = 0.50$ ,  $p = 0.01$ ) but not with IPN number ( $\rho = 0.11$ ,  $p = 0.60$ ). The  $ID_{IMVF}/ID_l$  ratio was not correlated with either IPN number ( $\rho = -0.27$ ,  $p = 0.20$ ) or area ( $\rho = 0.04$ ,  $p = 0.84$ ). There was a significant correlation between CEUS results and IPN in carotid plaques, but not between SMI and IPN. Further studies are needed to confirm these findings.

**Key words** : carotid artery, contrast-enhanced ultrasonography,  
intraplaque neovascularization, superb microvascular imaging

**I. Introduction**

Intraplaque neovascularization (IPN) in carotid artery atherosclerotic plaques is a

risk factor for atherothrombosis in patients with ischemic stroke<sup>1)</sup>. Contrast-enhanced ultrasonography (CEUS) of the carotid artery can be used to assess IPN<sup>2)</sup>. Recent studies have shown that high contrast enhancement in carotid plaques visualized by CEUS can

Corresponding author: Kazumasa Oura  
koura@iwate-med.ac.jp

reliably predict the presence of abundant neovascularization, plaque rupture, and intraplaque hemorrhage in histopathological specimens<sup>2,3</sup>). However, the problems with CEUS have been that the procedure is complicated, invasive, and not covered by public health insurance in Japan<sup>4</sup>). Superb microvascular imaging (SMI) is a novel ultrasound imaging technique developed to depict low-velocity blood flow without contrast agent<sup>4</sup>). SMI can differentiate true microvascular flow signals from artifacts and depict intraplaque microvascular flow (IMVF) signals<sup>5</sup>). We recently developed a quantitative assessment method for SMI and reported its usefulness for predicting microembolic signals during carotid endarterectomy (CEA)<sup>6</sup>). However, no comparison of quantitative data with pathological findings has been made. The purpose of this study was to compare the quantitative data of SMI and CEUS as a method of identifying IPN in tissue specimens obtained by CEA.

## II. Materials and Methods

### 1. Study population

This was a single-center prospective observational study. Participants were selected from consecutive patients who underwent CEA at our hospital from March 2017 to November 2018. We excluded patients based on the following criteria: 1) allergic to perflubutane or eggs<sup>7</sup>); 2) difficulty visualizing plaque with acoustic shadow due to calcification; 3) arrhythmias which inhibit analysis using time-intensity curves; or 4) other circumstances that make evaluation with SMI or CEUS difficult. This study was carried out in accordance with the guidelines

of the World Medical Association and the Declaration of Helsinki<sup>8</sup>). The protocol was approved by Iwate Medical University Ethics Committee (No. MH2019-061) and written informed consent was obtained from all patients or their next of kin before participation.

### 2. Carotid artery ultrasound

Carotid ultrasonography was performed with an Aplio 700i machine (Canon Medical Systems, Otawara, Japan) and an 18-MHz linear probe by a single investigator (a registered neurosonographer of the Japan Academy of Neurosonology) 3 days before CEA.

### 3. Superb microvascular imaging ultrasonography

SMI ultrasonography was performed using the monochrome SMI mode after identifying the carotid plaque using B mode or color doppler mode images. Twin-views display of plaques in B-mode and monochrome SMI were displayed side-by-side with electrocardiogram gating<sup>6</sup>). The region of interest (ROI) box of SMI was placed around the entire plaque with a mechanical index of 1.0, frame rate of 28 frames/s, dynamic range of 65 dB, and SMI velocity of 1.5 cm/s. We observed the carotid plaques for 2 min on the longitudinal view<sup>6</sup>). Static enhancement was visually excluded by one examiner who was blinded to patient information, and the IMVF signal was identified as a mobile enhancement in the plaques on SMI images (Fig. 1A, arrow). The circular ROI were manually placed to include the IMVF signals when IMVF signals were identified within the plaque (Fig. 1B, yellow circle). ROI were placed in all these signals when 2 or more IMVF signals were identified within the carotid plaque. When IMVF signals

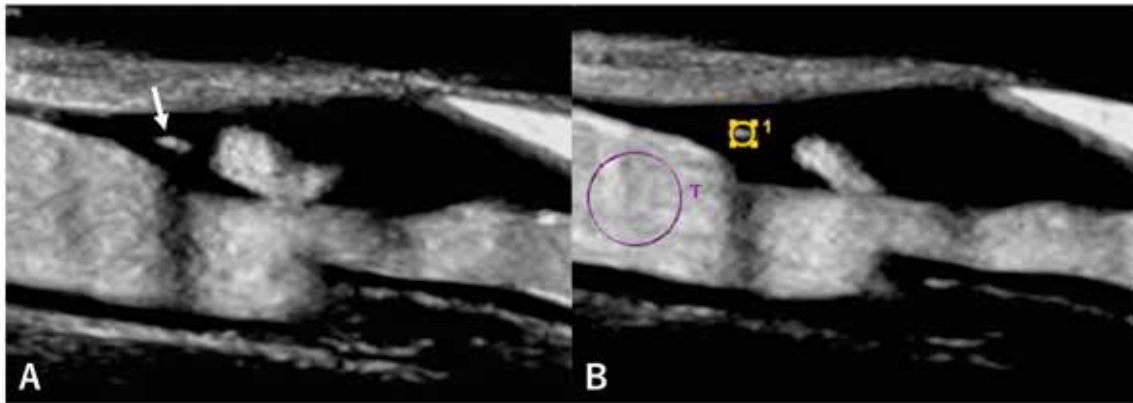


Fig. 1. Superb microvascular imaging of carotid plaque.

- (A) Intraplaque microvascular flow signals moving towards the plaque core and lumen (white arrow).
- (B) Each region of interest was set at the intraplaque microvascular flow signal within the carotid plaque (yellow circle) and at the center within the lumen of the carotid artery proximal to the stenotic lesion (purple circle), respectively.

were not identified within the carotid plaque, we arbitrarily placed 2 circular ROI near the carotid plaque surface within the plaque so those ROI did not include static enhancements. Regions with acoustic shadows due to calcification were excluded from the ROI. Next, a circular ROI was manually placed in the center of the lumen of the carotid artery proximal to the stenosis on the same image (Fig. 1B, purple circle). After that, these signal data from the SMI ultrasound examinations were transferred to the workstation. Time-intensity curves of the IMVF signal (arbitrary ROI signals were defined as IMVF signals when there were no visually identified IMVF signals within the carotid plaque) and lumen ROI were generated using in-house software on MAT-LAB R2015b (MathWorks, Natick, MA). After selecting 10 heartbeat cycles from both time-intensity curves, each heartbeat cycle was segmented based on gated electrocardiogram findings. Then we selected 10 heartbeat cycles from both time-intensity curves and segmented each heartbeat cycle

based on gated electrocardiogram findings. The durations of all 10 segmented time-intensity curves were made uniform since the duration of each heartbeat cycle differs slightly because of respiratory fluctuation and autonomic nerve function, even in healthy patients (Fig. 2A). These 10 uniform segmented time-intensity curves were then averaged with respect to the IMVF signal and luminal ROI (Fig. 2B). The difference between the 2 intensities (maximum intensity - minimum intensity; ID) was calculated based on the averaged IMVF signal ( $ID_{IMVF}$ ) and lumen ( $ID_l$ ) curves (Fig. 2C). Finally, the ratio of  $ID_{IMVF}$  to  $ID_l$  was calculated to account for the effect of the carotid lumen signal on the IMVF signal. The maximum  $ID_{IMVF}/ID_l$  ratio was selected for analysis when 2 or more ROI were placed within the carotid plaque in the same patient.

#### 4. Contrast-enhanced ultrasonography

After switching the examination mode to differential contrast harmonic imaging mode, the same area was visualized with CEUS.

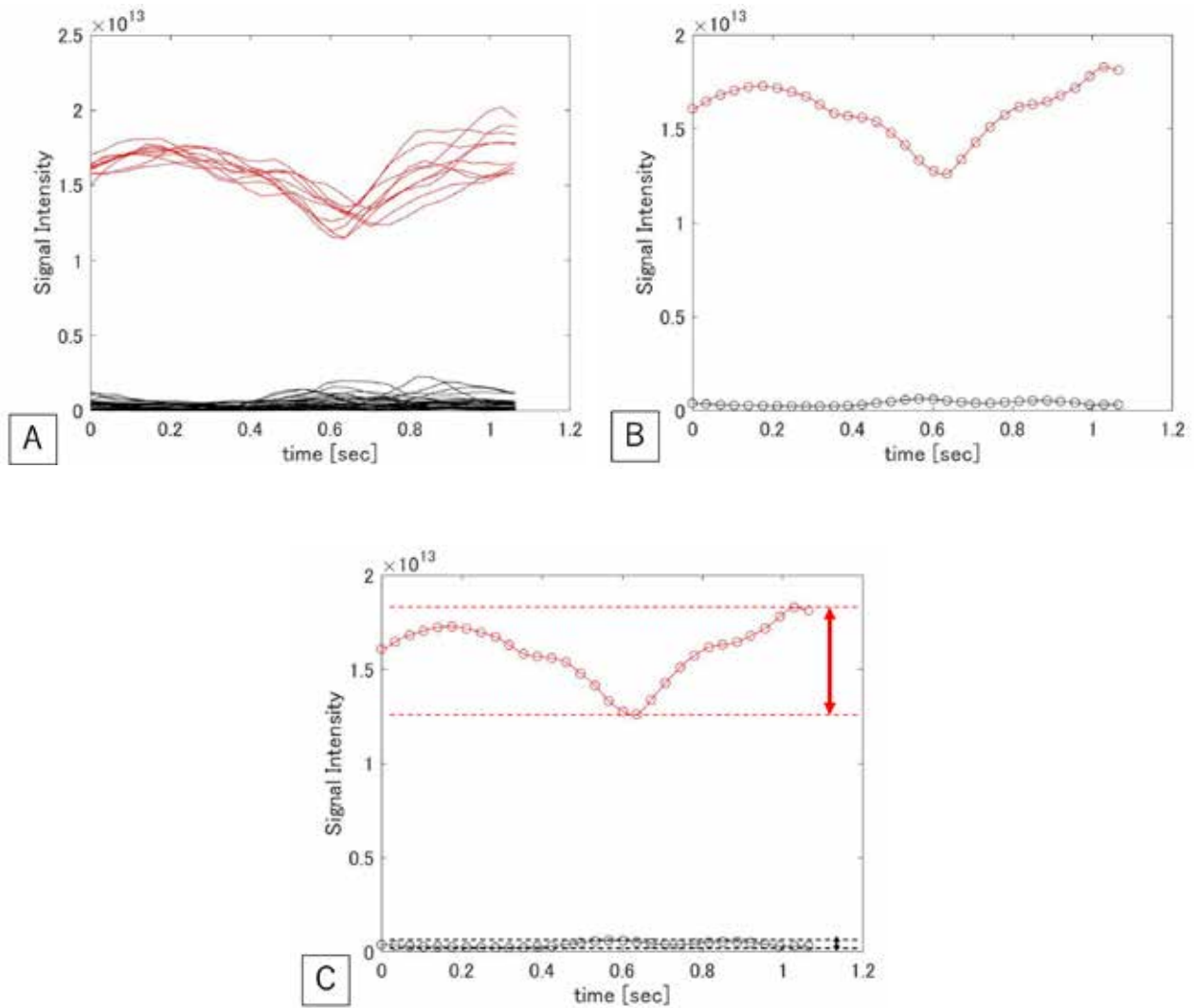


Fig. 2. Time-intensity curves of the intra-plaque microvascular flow signal and lumen.

The black and red lines indicate the time-intensity curves of the IMVF signal and lumen ROI, respectively. (A) The time-intensity curves of the IMVF signal and lumen ROI are segmented into 10 heartbeat cycles and the durations of all 10 segmented time-intensity curves were made uniform. (B) These 10 segmented and uniformed time-intensity curves were averaged with respect to the IMVF signal and lumen ROI. (C) The maximum and minimum intensities were determined (dotted lines) and the difference between the 2 intensities (maximum intensity–minimum intensity; ID) was calculated on the averaged IMVF signal (IDIMVF) and lumen (IDI) curves (vertical bidirectional arrow). IMVF; intraplaque microvascular flow, ROI; region of interest.

The CEUS imaging was performed with a mechanical index of 0.19 to 0.26, frame rate of 15 to 20 frames/s, and dynamic range of 35 to 65 dB. As previously reported, perflubutane was used as the contrast agent and was administered by bolus at 0.01 ml/kg body

weight<sup>4)</sup>. Carotid plaques were observed on the longitudinal plane for 70 sec (Fig. 3A). As with SMI, the ROIs were manually placed by a single investigator who was blinded to patient information. If there was an inflow of contrast agent into the plaque, the ROI was placed to

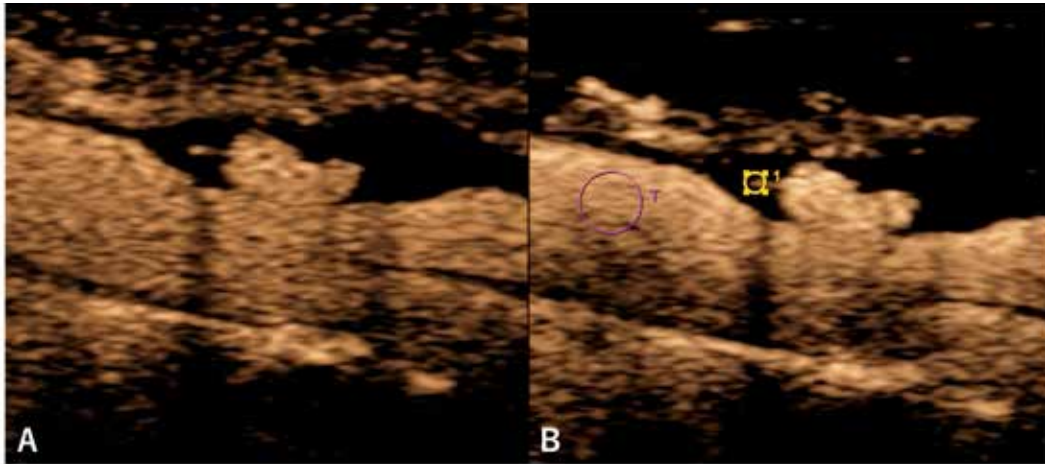


Fig. 3. Contrast-enhanced ultrasonography of carotid plaque.

The ROI was placed to include the contrast-enhanced area in the plaque (yellow circle) and in the center of the vessel lumen proximal to the stenosis (purple circle). ROI; region of interest.

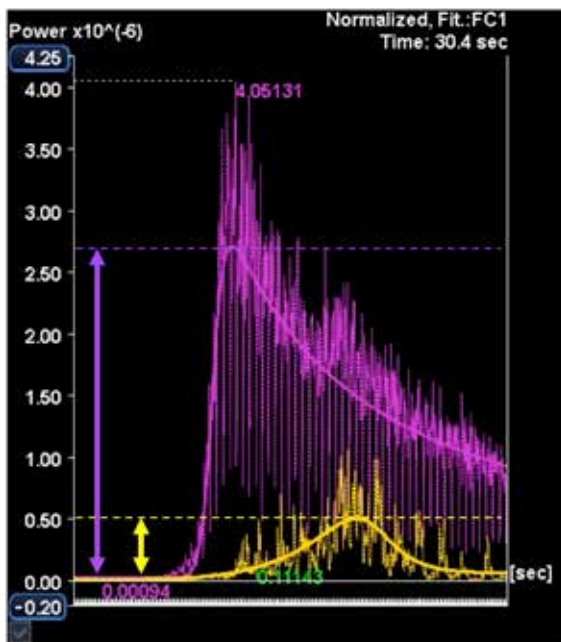


Fig. 4. Time-intensity curve of contrast-enhanced ultrasonography.

The yellow line indicates the degree of contrast effect in the plaque and the purple line indicates the degree of contrast effect in the vessel lumen. Yellow bidirectional arrow indicates enhanced intensity in the core. Purple bidirectional arrow indicates enhanced intensity of the vessel.

include the contrast-enhanced area (Fig. 3B, yellow circle) and if there was no inflow of

contrast medium, a single circular ROI was arbitrarily placed in the plaque. The ROIs were placed to exclude areas with calcification or static enhancement signals. The same investigator then placed a circular ROI in the center of the vessel lumen proximal to the stenosis, on the same image (Fig. 3B, purple circle). Time-intensity curves were created for ROIs in the plaque and in the vessel lumen using an application on the ultrasound device. The baseline intensity before contrast injection and the maximum intensity after injection were calculated as the intraplaque and luminal curves for each patient. The enhanced intensity (EI) was calculated by subtracting the baseline intensity from the maximum intensity of the intraplaque ( $EI_p$ ) and intraluminal curves ( $EI_l$ ) (Fig. 4). The ratio of  $EI_p$  to  $EI_l$  was then calculated for each patient<sup>6</sup>.

#### 5. Histological examination

Plaques removed by CEA were cut into 5 mm pieces, formalin-fixed, and paraffin-embedded. The specimens were cut at a

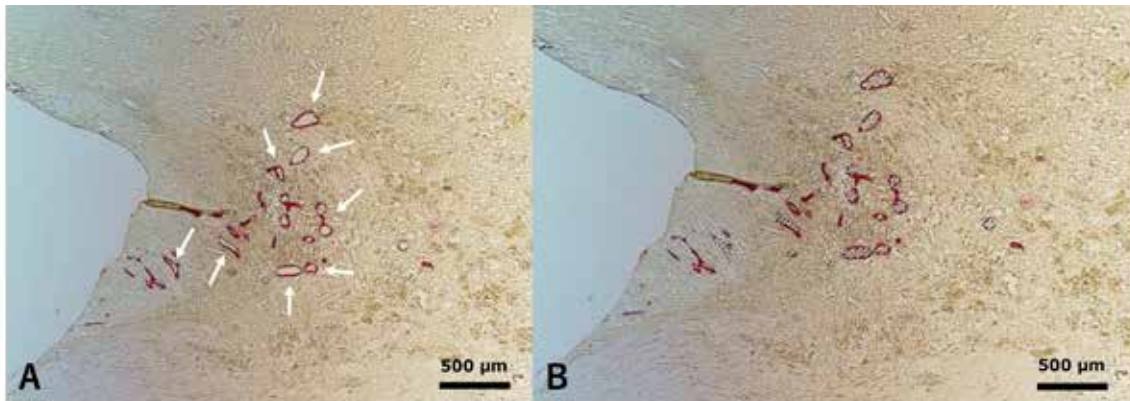


Fig. 5. Neovascularization stained with anti-CD34 antibody.

All sections were observed at 40x magnification.

(A) The vessels that retained their luminal structure were selected and the lumen area was calculated (white arrows).

(B) The area enclosed by the dotted line was included in the study.

thickness of  $7\mu\text{m}$  for short-axis images. The sections were immunostained with anti-CD34 antibody, which stains vascular endothelium, and IPN was defined as the presence of endothelial cells in a circular shape and a visible vascular lumen. All slices were observed at 40x magnification, and the slice including the areas with the highest concentration of neovascularization were visually identified by 1 investigator. The number of neovessels (IPN number) and the area of the lumen of neovessels (IPN area) was evaluated by 2 investigators who were blinded to patient information. The IPN area was calculated using bitmap image editing software (Adobe Photoshop; Adobe, San Jose, United States) (Fig. 5A, B). The mean values of the IPN number and the area measured by 2 investigators were used for further analysis.

#### 6. Statistical analysis

SPSS version 26 (IBM Japan, Tokyo, Japan) was used for all statistical analysis. Spearman's rank correlation coefficient was used to calculate the correlation between the  $ID_{IMVF}/$

$ID_I$  ratio or the  $EI_p/EI_I$  ratio and the number or the area of neovascularization on tissue samples. Continuous variables were expressed as medians and interquartile ranges (IQRs), then analyzed using the Mann-Whitney U test since some continuous variables were not normally distributed. The inter-rater reliability of determining neovascularization in tissue specimens was examined by 2 evaluators using the intraclass correlation coefficient ICC (2, 1). ICC (2, 1) is a reliability index used to

Table 1. Clinical characteristics

Variable	Value (n = 25)
Age (years), median [IQR]	70 [66 - 76]
Male, n (%)	25 (100)
Symptomatic lesion, n (%)	23 (92)
Hypertension, n (%)	21 (84)
Diabetes mellitus, n (%)	6 (24)
Dyslipidemia, n (%)	20 (80)
Degree of stenosis (%), median [IQR]	90 [80 - 95]

n; number, IQR; interquartile range.



Table 2. Ultrasound findings and intraplaque neovascularization

	CEUS			SMI		
	Contrast effect (+)	Contrast effect (-)	p-value	IMVF (+)	IMVF (-)	p-value
Number of IPN (n), median [IQR]	11 [3-20]	17 [9-20]	0.77	6 [3-14]	19 [10-20]	0.06
Area of IPN (pixel), median [IQR]	16,006 [7613-19,566]	8085 [4004-11,483]	0.08	8735 [3582-18,567]	10,060 [7613-16,006]	0.89

n; number, IPN; intraplaque neovascularization, IQR; interquartile range, CEUS; contrast-enhanced ultrasonography, SMI; superb microvascular imaging, IMVF; intraplaque microvascular flow.

Table 3. Correlation of EIp/EI<sub>l</sub> ratio on contrast-enhanced ultrasonography and ID<sub>IMVF</sub>/ID<sub>l</sub> ratio on superb micro-vascular imaging findings and intraplaque neovascularization in tissue specimens.

	EIp/EI <sub>l</sub> ratio		ID <sub>IMVF</sub> /ID <sub>l</sub> ratio	
	$\rho$	p-value	$\rho$	p-value
Number of IPN	0.11	0.60	- 0.27	0.20
Area of IPN (pixel)	0.50	0.01	0.04	0.84

IPN; intraplaque neovascularization, EIp; enhanced intensity of intraplaque, EI<sub>l</sub>; enhanced intensity of intraluminal, ID; The difference between the 2 intensities (maximum intensity – minimum intensity), IMVF; intraplaque microvascular flow, ID<sub>IMVF</sub>; ID calculated based on averaged IMVF, ID<sub>l</sub>; ID calculated based on averaged lumen.

generalize reliability results to two raters with the same characteristics<sup>9)</sup>.

### III. Results

#### 1. Clinical characteristics

Although we screened 50 patients, 17 were excluded because of poor plaque visualization due to severe calcification, 4 were excluded because of inability to stay still or artifacts, and 4 were excluded because of arrhythmias. Therefore, 25 patients were enrolled in this study (Table 1).

#### 2. Ultrasound findings and intraplaque neovascularization

The median IPN number on tissue specimens

was 15 [IQR, 4 - 20] and the median IPN area was 10,060 pixels [IQR, 5710 - 17,229]. The ICC (2, 1) of histological examination was good at 0.97.

IMVF signals on SMI were identified in 8 of 25 patients (32%), and contrast effects on CEUS were identified in 13 of 25 patients (52%).

There were no significant differences in the IPN number or the IPN area with or without the IMVF signals on SMI imaging and contrast effect on CEUS (Table 2).

#### 3. Correlation of EIp/EI<sub>l</sub> ratio on contrast-enhanced ultrasonography and ID<sub>IMVF</sub>/ID<sub>l</sub> ratio on superb micro-vascular imaging

findings and intraplaque neovascularization in tissue specimens

The  $EI_p/EI_l$  ratio on CEUS was significantly correlated with the area of IPN ( $\rho = 0.50$ ,  $p = 0.01$ ). However, there was no significant correlation between the  $EI_p/EI_l$  ratio and the IPN number ( $\rho = 0.11$ ,  $p = 0.60$ ). The  $ID_{IMVF}/ID_l$  ratio was not correlated with either the IPN number ( $\rho = -0.27$ ,  $p = 0.20$ ) or area ( $\rho = 0.04$ ,  $p = 0.84$ ) (Table 3).

#### IV. Discussion

In this study, we compared the usefulness of SMI with that of CEUS for predicting IPN on tissue specimens obtained by CEA. Although the  $EI_p/EI_l$  ratio of CEUS showed a significant correlation with the area of IPN on tissue specimens, carotid ultrasonography using SMI did not show significant correlation with pathological findings of IPN.

We previously reported that preoperative CEUS for CEA could predict intraoperative microembolic signals<sup>7)</sup>. In addition, many previous studies have used CEUS to observe intraplaque neovascularization<sup>2,10-12)</sup>. However, contrast agent for carotid ultrasonography is not covered by Japanese public health insurance, and the possibility of allergic or adverse reactions to contrast agents would make it difficult to use CEUS as a standard modality to evaluate IPN in carotid plaques<sup>4)</sup>. Recently, several studies have reported the usefulness of SMI to evaluate IPN in carotid plaques<sup>4-6)</sup>. Visual determination of IMVF signals using SMI is reported to be associated with the IPN number in tissue specimens<sup>14,15)</sup>. However, both visual determination of IMVF signal is based on semi-quantitative evaluation. No study has yet examined the

association between quantitative data and the IPN number in tissue specimens. One of the objectives of this study was to show the association between quantitative data of SMI and quantitative data of IPN. However, we could not show an association between the findings of SMI and IPN in tissue specimens in this study.

Previous reports either analyzed all slices of carotid plaques or, as we did in the present study, used the area with the highest IPN number for analysis<sup>5,16)</sup>. Our method was based on the "hot spot method" presented by Weidner, Folkman et al.<sup>17,18)</sup>. However, this method is prone to bias depending on the observer. Fox et al. established the Chalkley count to reduce this bias. The Chalkley count is the number of grid points that hit stained vessels, taken as an average from the assessment of three hot spots. However, it is somewhat complicated, which is a drawback. In the present study, the emphasis was on a simpler evaluation, so the usual "hot spot method" was used. Moreover, because the resolution of the 18-MHz linear probe which was used for SMI in this study is  $500\mu\text{m}$ , vessels smaller than  $500\mu\text{m}$  would not be delineated by SMI. Therefore, the IMVF signal intensity may depend on the size of neovessels. We measured the area of IPN on tissue specimens, but did not measure the size of individual neovessels. The number of neovessels of a certain size may be related to the signal intensity of IMVF.

Another method of quantification is the assessment of neovascularization by fluorescence imaging<sup>19)</sup>. Although fluorescence imaging is cumbersome and thus falls short of the goal of simple evaluation, it is an option that should



be considered.

Previous reports have evaluated the signal strength of SMI in a semi-quantitative manner<sup>16)</sup>. Chen et al. reported a positive correlation between semiquantitative data of SMI and neovascular density<sup>16)</sup>. Our study was quantified using the methodology used to assess the IMVF signals on SMI in a previous study<sup>6)</sup>. However, in the present study, we were unable to demonstrate an association with IPN. Alternative quantification methods may need to be investigated. Some reports have quantified SMI by other methods in thyroid evaluation<sup>20,21)</sup>, and the method may be used to evaluate IPN. It is also unclear whether the lesion where intraplaque blood flow was detected by CEUS or SMI was the same as the lesion evaluated in the tissue specimen. Chen et al. make a similar point, stating that bias cannot be completely ruled out<sup>16)</sup>.

Several studies have reported the usefulness of 3D ultrasound systems in the carotid region<sup>22-27)</sup>. In the past, the cost of 3D ultrasound probes and the need for a dedicated laboratory made them less popular. In recent years, however, new technologies have been developed that allow for easy implementation of 3D ultrasound. The 3D ultrasound system has the potential to solve this problem.

There are some limitations in the present study. First, the sample size was small. Exclusion due to poor visualization on

ultrasound might be unavoidable when evaluating the usefulness of carotid ultrasonography. So it will be necessary to expand the sample size in future studies. Second, the examiner visually distinguished the IMVF signals or contrast enhancement from other static enhancements such as intraplaque calcification. It is difficult to make these discriminations visually. Therefore, bias cannot be completely eliminated by the methods used in this study. The development of an automated and more accurate method of identifying IMVF signals would allow more reliable assessment of IPN.

## V. Conclusion

There was a significant correlation between the  $EI_p/EI_l$  ratio of CEUS and the IPN area in carotid plaques, but not between the  $ID_{IMVF}/ID_l$  ratio of SMI and the IPN number or area. Further studies using more quantitative assessment in a larger patient population are warranted to confirm the association between SMI findings and IPN in carotid plaques.

### Acknowledgement

We thank Leah Cannon, PhD, from Edanz (<https://jp.edanz.com/ac>) for editing a draft of this manuscript.

Conflict of interest: The authors have no conflict of interest to declare.

## References

- 1) **McCarthy MJ, Loftus IM, Thompson MM, et al.**: Angiogenesis and the atherosclerotic carotid plaque: an association between symptomatology and plaque morphology. *J Vasc Surg* **30**, 261-268, 1999.
- 2) **Saito K, Nagatsuka K, Ishibashi-Ueda H, et al.**: Contrast-enhanced ultrasound for the evaluation of neovascularization in atherosclerotic carotid artery plaques. *Stroke* **45**, 3073-3075, 2014.
- 3) **Staub D, Partovi S, Schinkel AF, et al.**: Correlation

- of carotid artery atherosclerotic lesion echogenicity and severity at standard US with intraplaque neovascularization detected at contrast-enhanced US. *Radiology* **258**, 618-626, 2011.
- 4) **Oura K, Kato T, Ohba H, et al.**: Evaluation of intraplaque neovascularization using superb microvascular imaging and contrast-enhanced ultrasonography. *J Stroke Cerebrovasc Dis* **27**, 2348-2353, 2018.
  - 5) **Zamani M, Skagen K, Scott H, et al.**: Carotid plaque neovascularization detected with superb microvascular imaging ultrasound without using contrast media. *Stroke* **50**, 3121-3127, 2019.
  - 6) **Chiba T, Fujiwara S, Oura K, et al.**: Superb microvascular imaging ultrasound for cervical carotid artery stenosis for prediction of the development of microembolic signals on transcranial doppler during carotid exposure in endarterectomy. *Cerebrovasc Dis Extra* **11**, 61-68, 2021.
  - 7) **Oikawa K, Kato T, Oura K, et al.**: Pre-operative cervical carotid artery contrast-enhanced ultrasound findings are associated with development of microembolic signals on transcranial doppler during carotid exposure in endarterectomy. *Atherosclerosis* **260**, 87-93, 2017.
  - 8) World Medical Association: World Medical Association Declaration of Helsinki ethical principles for medical research involving human subjects. *JAMA* **310**, 2191-2194, 2013.
  - 9) **Koo TK and Li MY**: A guideline of selecting and reporting intraclass correlation coefficients for reliability research. *J Chiropr Med* **15**, 155-163, 2016.
  - 10) **Huang R, Abdelmoneim S, Ball CA, et al.**: Detection of carotid atherosclerotic plaque neovascularization using contrast enhanced ultrasound: a systematic review and meta-analysis of diagnostic accuracy studies. *J Am Soc Echocardiogr* **29**, 491-502, 2016.
  - 11) **Owen DR, Shalhoub J, Miller S, et al.**: Inflammation within carotid atherosclerotic plaque: assessment with late-phase contrast-enhanced US. *Radiology* **255**, 638-644, 2010.
  - 12) Superb Micro-vascular Imaging (SMI). Canon Medical Systems (2014, accessed 23 October 2019). <https://jp.medical.canon/News/PressRelease/Detail/12145-834>.
  - 13) **Miyamoto Y, Ito T, Takada E, et al.**: Efficacy of sonazoid (perflubutane) for contrast-enhanced ultrasound in the differentiation of focal breast lesions: phase 3 multicenter clinical trial. *Am J Roentgenol* **202**, 400-407, 2014.
  - 14) **Zhang H, Du J, Wang H, et al.**: Comparison of diagnostic values of ultrasound micro-flow imaging and contrast-enhanced ultrasound for neovascularization in carotid plaques. *Exp Ther Med* **14**, 680-688, 2017.
  - 15) **Zhu YC, Jiang XZ, Bai QK, et al.**: Evaluating the efficacy of atorvastatin on patients with carotid plaque by an innovative ultrasonography. *J Stroke Cerebrovasc Dis* **28**, 830-837, 2019.
  - 16) **Chen X, Wang H, Jiang Y, et al.**: Neovascularization in carotid atherosclerotic plaques can be effectively evaluated by superb microvascular imaging (SMI): initial experience. *Vasc Med* **25**, 328-333, 2020.
  - 17) **Weidner N, Semple JP, Welch WR, et al.**: Tumor angiogenesis and metastasis-correlation in invasive breast carcinoma. *N Engl J Med* **324**, 1-8, 1991.
  - 18) **Fox SB, Leek RD, Weekes MP, et al.**: Quantitation and prognostic value of breast cancer angiogenesis: comparison of microvessel density, Chalkey count, and computer image analysis. *J Pathol* **177**, 275-283, 1995.
  - 19) **Hanyu A, Kojima K, Hatake K, et al.**: Functional in vivo optical imaging of tumor angiogenesis, growth, and metastasis prevented by administration of anti-human VEGF antibody in xenograft model of human fibrosarcoma HT1080 cells. *Cancer Sci* **100**, 2085-2092, 2009.
  - 20) **Russ G, Bonnema SJ, Erdogan MF, et al.**: European Thyroid Association Guidelines for ultrasound malignancy risk stratification of thyroid nodules in adults: the EU-TIRADS. *Eur Thyroid J* **6**, 225-237, 2017.
  - 21) **Hong MJ, Ahn HS, Ha SM, et al.**: Quantitative analysis of vascularity for thyroid nodules on ultrasound using superb microvascular imaging: can nodular vascularity differentiate between malignant and benign thyroid nodules? *Medicine (Baltimore)* **101**, 1-9, 2022.
  - 22) **van Engelen A, Wannarong T, Parraga G, et al.**: Three-dimensional carotid ultrasound plaque texture predicts vascular events. *Stroke* **45**, 2695-2701, 2014.
  - 23) **Kozàková M, Morizzo C, Andreucetti F, et al.**: Quantification of extracranial carotid artery stenosis by ultrafast three-dimensional ultrasound. *J Am Soc Echocardiogr* **14**, 1203-1211, 2001.

- 24) **Pelz JO, Weinreich A, Fritzsich D, et al.:** Quantification of internal carotid artery stenosis with 3D ultrasound angiography. *Ultraschall Med* **36**, 487-493, 2015.
- 25) **Chiu B, Beletsky V, Spence JD, et al.:** Analysis of carotid lumen surface morphology using three-dimensional ultrasound imaging. *Phys Med Biol* **54**, 1149-1167, 2009.
- 26) **Vicenzini E, Galloni L, Ricciardi MC, et al.:** Advantages and pitfalls of three-dimensional ultrasound imaging of carotid bifurcation. *Eur Neurol* **65**, 309-316, 2011.
- 27) **Igase K, Kumon Y, Matsubara I, et al.:** Utility of 3-dimensional ultrasound imaging to evaluate carotid artery stenosis: comparison with magnetic resonance angiography. *J Stroke Cerebrovasc Dis* **24**, 148-153, 2015.

## 頸動脈プラーク内新生血管の評価における superb microvascular imaging と 造影超音波検査の比較

清川哲郎<sup>1)</sup>, 大浦一雅<sup>1)</sup>, 千葉貴之<sup>2)</sup>,  
藤原俊朗<sup>2)</sup>, 板橋 亮<sup>1)</sup>, 小笠原邦昭<sup>2)</sup>,  
人見次郎<sup>3)</sup>, 前田哲也<sup>1)</sup>

<sup>1)</sup> 岩手医科大学医学部, 内科学講座脳神経内科・老年科分野

<sup>2)</sup> 岩手医科大学医学部, 脳神経外科学講座

<sup>3)</sup> 岩手医科大学医学部, 解剖学講座人体発生学分野

*(Received on January 10, 2023 & Accepted on February 14, 2023)*

### 要旨

頸動脈プラーク内新生血管 (IPN) を評価するための superb micro-vascular imaging (SMI) と造影超音波検査 (CEUS) を比較検討した。70% 以上の頸動脈内膜切除術を受けた患者 25 名を登録した。SMI により頸動脈プラーク内の微小血流 (IMVF) 信号を評価し, IMVF 信号強度の最大値と最小値の差 ( $ID_{IMVF}$ ) と内腔の信号強度 ( $ID_1$ ) の比を算出した。また, CEUS で造影強度を測定し, プラーク内強度の最大値とベースライン値の差 ( $EI_p$ ) と管腔内曲線 ( $EI_1$ ) の比を算出した。抗 CD34 抗体で染

色した組織切片で IPN 数, 面積を測定した。8 名で IMVF 信号を, 13 名で造影効果を認めた。 $EI_p/EI_1$  比は IPN 面積と有意な相関があったが ( $\rho = 0.50, p = 0.01$ ), IPN 数とは相関がなかった ( $\rho = 0.11, p = 0.60$ )。  $ID_{IMVF}/ID_1$  比は IPN 数 ( $\rho = -0.27, p = 0.20$ ), 面積 ( $\rho = 0.04, p = 0.84$ ) のいずれとも相関がなかった。頸動脈プラークにおける CEUS の結果と IPN の間には有意な相関があったが, SMI と IPN の間には相関がなかった。これらの知見を確認するためにはさらなる研究を要する。